Theoretical Investigation of ^{19}F NMR Chemical Shielding Tensors in Fluorobenzenes

Lori K. Sanders and Eric Oldfield*

Department of Chemistry, University of Illinois at Urbana-Champaign, 600 South Mathews Avenue, Urbana, Illinois 61801

Received: March 26, 2001

We report the theoretical ^{19}F NMR shielding tensor magnitudes and orientations for a series of fluoroaromatic species, together with a comparison with experimental results. We discuss results for Hartree−Fock (HF) and second-order Møeller−Plesset theory (MP2) geometry optimized structures and HF-gauge including atomic orbitals (HF-GIAO), sum over states-density functional theory-independent gauges for localized orbitals (SOS-DFT-IGLO) and MP2-GIAO shielding calculations, for several basis set arrangements. In general, MP2 and DFT methods show few improvements over HF methods, at the expense of time (MP2) and accuracy (MP2 and DFT). Pure density functionals overestimate the tensor breadths (spans), an effect that is only partially offset by use of hybrid exchange correlation functionals. HF-GIAO methods in general give good overall predictions of ^{19}F shielding tensor elements. In the case of potassium tetrafluorophthalate, we also demonstrate that use of the charge field perturbation-IGLO technique provides accurate shielding tensor elements, as well as accurate shielding tensor orientations. We also report the calculation of the shielding derivatives, $\partial\sigma_{ii}/\partial r$, for the ^{19}F nucleus in fluorobenzene (and HF) and the ^{1}H nucleus in benzene. Surprisingly, the derivative along the C−F bond axis ($\partial\sigma_{22}/\partial r$) is quite large, 460 ppm Å^{-1}, unlike that expected and found in HF, or in benzene, indicating a strong p-orbital interaction with the benzene ring. The ^{19}F shielding tensor results are thus quite sensitive to the actual bond lengths employed (derived from geometry optimizaitons), with MP2 optimization permitting the best accord with experiment. Overall, MP2 optimization and HF-GIAO shielding tensor calculations were found to give the best results, consistent with previous isotropic chemical shift/shielding results.

Introduction

Fluorine-19 nuclear magnetic resonance (NMR) investigations have been of interest for many years, due in large part to the experimentally attractive properties of ^{19}F, including 100% natural abundance, spin $I = {}^1/_2$ and a large magnetogyric ratio. Indeed, many of the early discoveries of *J*-couplings and chemical shifts involved the ^{19}F nucleus, and in more recent years, ^{19}F has been used as a probe of macromolecular structure, where the large chemical shift range of ^{19}F has enabled well-resolved spectra of ^{19}F-labeled proteins to be investigated.[1,2] These studies have been accompanied by theoretical investigations of ^{19}F shielding[3] and *J*-couplings,[4] and there has been considerable interest in using both ab initio quantum chemical and density functional theory (DFT) methods to investigate shifts (or shielding) in both simple and quite complex systems.[3,4]

In early work, de Dios and Oldfield[3] utilized ab initio methods to investigate the large range of isotropic chemical shifts and chemical shift tensor elements in a series of fluorobenzenes. Using a Hartree−Fock self-consistent field with gauge including atomic orbitals (SCF-GIAO) method,[5,6] these workers found that experimental ^{19}F NMR chemical shifts and shift (shielding) tensor elements were quite well correlated with experimental values. More recently, Webb and co-workers have made more detailed investigations of the effects of electron correlation and basis sets on geometry optimization and ^{19}F chemical shielding in fluorobenzenes.[7,8] These authors reported that inclusion of dynamic electron correlation was necessary for accurate geometry optimization but found the MP2-GIAO method to overestimate the experimental chemical shifts, an effect also noted by Fukui.[9] Webb and co-workers also observed that an extension of basis sets in DFT GIAO calculations (using a B3LYP functional) impaired the quality of the calculations. Their work did not, however, report the effects of electron correlation and basis sets on either the magnitudes or orientations of the individual shielding tensor elements, which is thought by many to be a more stringent test of theory since there is less likely to be any fortuitous cancellation of errors. Consequently, we have investigated the effects of geometry optimization, electron correlation, and basis set effects on both the magnitudes and the orientations of individual chemical shielding tensor elements in a series of fluorobenzenes. The results are of general interest in the context of our current investigations of ^{13}C and ^{19}F shielding in proteins and model systems in which HF-GIAO methods have, for the most part, been used.

Computational Methods

The results described in this paper were obtained by using several different approaches. In the first, we used the coupled sum-over-states density functional perturbation theory with individual gauges for localized orbitals (SOS-DFPT-IGLO) approach using the program deMon-KS3p2[10−12] for NMR shielding calculations. Second, we carried out Hartree−Fock gauge including atomic orbitals (HF-GIAO), second-order Møeller−Plesset-GIAO (MP2-GIAO)[13−15] and uncoupled[16] DFT-GIAO shielding calculations using Gaussian 98.[17] Several basis set schemes were used, to compare our results with those

* To whom correspondence should be addressed. Fax: (217) 244-0997. E-mail: eo@chad.scs.uiuc.edu.

10.1021/jp011114f CCC: $20.00
Published on Web 08/03/2001

TABLE 1: Slope and R^2 Values of Theoretical[a] vs Experimental ^{19}F Chemical Shielding Tensor Elements for HF- and MP2-Optimized Fluorobenzenes[b]

optimization method	NMR method	σ_{11}		σ_{22}		σ_{33}		σ_{ii}		σ_{iso}[c]	
		slope	R^2	slope	R^2	slope	R^2	slope	R^2	slope	R^2
HF	HF	0.97	0.93	0.27	0.09	0.88	0.9	0.98	0.99	0.99	0.99
MP2	HF	1.10	0.98	1.10	0.83	0.83	1.00	0.91	0.98	0.89	0.98
MP2	MP2	0.80	0.96	0.31	0.15	1.07	1.00	0.90	0.99	0.99	0.99

[a] The absolute shielding tensors are presented in the Supporting Information, Tables S1−S3. [b] NMR calculations employed a locally dense 6-311++G(2d,2p)/6-311G basis set. Experimental data is from ref 29. [c] The slope and R^2 values for the isotropic shielding were plotted from all theoretical values and solution NMR data presented in ref 8 and references therein.

of previous workers.[3,7,8] All Hartree−Fock and MP2 geometry optimizations utilized a uniform 6-31G(d,p) basis set.[18]

For the coupled SOS-DFPT-IGLO shielding calculations, we used an IGLO-III[19] basis on all atoms together with a Becke88[20] exchange functional and a gradient corrected functional PW91.[21,22] A second set of SOS-DFPT-IGLO calculations employed the PW91[21,21] exchange functional as well as the PW91[21,22] correlation functional with an IGLO-III[19] basis. The DFT-GIAO shielding calculations in Gaussian 98 utilized either the Becke88 exchange functional[20] and the PW91[21,22] correlation functional (BPW91) or Becke's three-parameter hybrid functional[23] and the Lee, Yang, and Parr correlation functional (B3LYP).[24] The DFT-GIAO shielding calculations employed two basis set schemes, a uniform 6-311++G(2d,2p) basis or a locally[25] dense 6-311++G(2d,2p)/6-311G(d,p) basis set. All shielding values used in data analysis are included in the Supporting Information.

The HF-GIAO shielding calculations employed three different basis set schemes. The first was a locally dense[25] 6-311+G(2d) basis on fluorine and 6-311G(d,p) on carbon and hydrogen, corresponding to the scheme used by de Dios and Oldfield.[3] The MP2-GIAO calculations, as well as one set of HF-GIAO calculations, employed a locally dense 6-311++G(2d,2p)/6-311G(d,p) basis. Finally, a full 6-311++G(2d,2p) basis set on all atoms was also used for an additional set of HF-GIAO and DFT-GIAO shielding calculations.

Finally, we employed a charge field perturbation (CFP) approach[26,27] to investigate the effect of electrostatic fields in the case of the tetrafluorophthalate dianion model. An explicit tetrafluorophthalate dianion was surrounded by a charge field based on 53 additional tetrafluorophthalate dianions as well as the appropriate potassium counterions. Point charges used to represent these species were obtained from a consistent valence force field (CVFF).[28] The point charge calculations were carried out in deMon-KS3p2 using the SOS-DFPT-IGLO method with an IGLO-III[19] basis on all explicit atoms together with the Becke88[20] exchange functional and a gradient-corrected PW91 correlation functional.[21,22]

The systems used for comparison with solid-state NMR shielding tensor data were monofluorobenzene, 1,2-difluorobenzene, 1,3-difluorobenzene, 1,4-difluorobenzene, 1,3,5-trifluorobenzene, 1,2,4,5-tetrafluorobenzene, hexafluorobenzene, 1,2,3,4-tetrafluorobenzene, potassium tetrafluorophthalate, tetrafluorophthalate, and 1,2,3,4-tetrafluoro-5,6-dimethylbenzene. Molecules used for additional comparisons with solution-state NMR data were 1,2,3-trifluorobenzene, 1,2,4-trifluorobenzene, 1,2,3,5-tetrafluorobenzene, and 1,2,3,4,5-pentafluorobenzene.

All calculations were carried out on IBM RS/6000 (model 3CT; IBM Corporation, Austin, TX) and Silicon Graphics Origin 200 (SGI, Mountain View, CA) computers in this laboratory and on the Silicon Graphics Origin 2000 and HP-Convex Exemplar SP-2000 (Hewlett-Packard Company, Palo Alto, CA) computers located in the National Computational Science Alliance (NCSA) in Urbana, IL. All structures were generated and visualized in Cerius2 4.0 (Molecular Simulations, Inc. San Diego, CA).

Results and Discussion

We first investigated the effects of different methods of geometry optimization on the magnitudes of the individual chemical shielding tensor elements in a series of fluorobenzenes. We show in Table 1 the slopes and R^2 values obtained by plotting the theoretical shieldings (Tables S1−S3) vs the solid-state NMR chemical shieldings[29] for seven fluorobenzenes. Also shown in Table 1 are the values generated from the solution NMR data presented in ref 8. We first chose to compare the HF geometry optimization results first reported by de Dios and Oldfield[3] with the MP2 optimization results reported by Webb and co-workers.[8] Although both groups reported favorable experimental vs theoretical isotropic chemical shift results, we find that the slopes and R^2 values of the HF-GIAO isotropic shielding calculation vs the experimental shift for MP2-optimized structures are slightly worse than when using the HF-optimized structures, when considering all of the solid state σ_{ii} values. There is no significant difference in the slopes and R^2 values for the solution state σ_{iso} values obtained from ref 8. The MP2 opt/HF-GIAO σ_{ii} values are in worse agreement with experiment than are the HF/HF-GIAO results, for both solid-state shielding tensor element and solution state isotropic chemical shift results.

Although the MP2 optimization does not appear to result in any *overall* improvement in calculation of σ_{ii} or σ_{iso} values, our results do show one interesting effect, which is that there is an improvement in the calculation of the σ_{22} tensor element for the MP2-optimized structures, as shown in Table 1. For example, the HF-GIAO NMR results show an improvement from a slope = 0.27 and R^2 = 0.09 to a slope = 1.10 and R^2 = 0.83. There is also a slight improvement seen in the correlations of σ_{11} and σ_{33}; however, the slopes of σ_{11} and σ_{33} are either unchanged or slightly worse. The improvement seen in the σ_{22} tensor element might be attributable to two factors. First, the σ_{22} shielding tensor element has the smallest experimental shift range of any of the three tensor elements. Consequently, even small changes in the theoretical (or experimental) tensor element values might produce a large difference in the statistics. Second, the σ_{22} tensor element might be rather susceptible to errors in C−F bond length. This second alternative would appear less likely since σ_{22} is along the C−F bond, and, at least in diatomics, would not be expected to change with changes in bond length. Nevertheless, since we are not dealing with diatomics, we calculated the ^{19}F NMR chemical shielding tensor elements of monofluorobenzene and, for comparison, HF as a function of bond length. In HF, the H−F bond length was increased systematically from 0.865 to 0.925 Å, while in C_6H_5F, the C−F bond length was increased from 1.330 to 1.366 Å, a range that includes the geometry-optimized bond lengths for both Hartree−

TABLE 2: Shielding Derivatives with Respect to Bond Length (ppm/Å^n)[a,b]

tensor element/ derivative order (n)	C_6H_5F HF-GIAO	C_6H_5F BPW91-GIAO	C_6H_5F B3LYP-GIAO	C_6H_6 HF-GIAO	H−F HF-GIAO
σ_{11} (1)	−220	−431	−372	−20	−578
σ_{11} (2)	−1615	−2341	−2222	70	−2026
σ_{22} (1)	424	485	480	3	−578
σ_{22} (2)	−1319	−923	−1068	−54	−2026
σ_{33} (1)	−588	−751	−718	−22	−4
σ_{33} (2)	−1745	2653	−2484	59	21
σ_{iso} (1)	−128	−232	−203	−14	−387
σ_{iso} (2)	−1558	−1972	−1924	24	−1343

[a] The derivatives represent the values ($\partial\sigma/\partial r$) and ($\partial^2\sigma/\partial^2 r$) and are given in units of ppm/Å and ppm/Å^2. [b] The absolute shielding tensors are presented in the Supporting Information, Tables S4−S8.

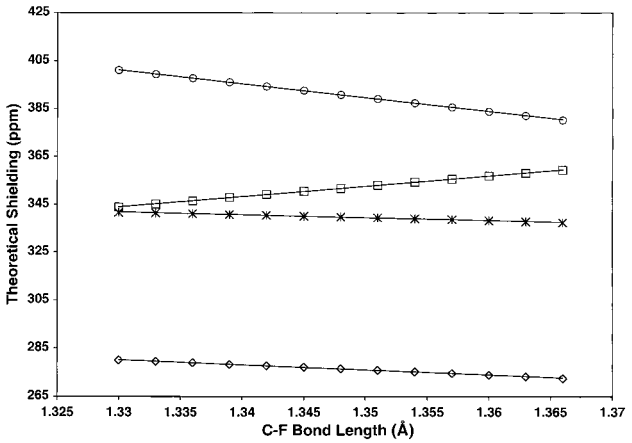

Figure 1. Graph showing the theoretical monofluorobenzene ^{19}F NMR chemical shielding tensor elements and isotropic shift as a function of C−F bond length: (◇) σ_{11}; (□) $\sigma_{22} = \sigma_{33}$, (*) $\sigma_{isotropic}$.

Fock (1.331 Å) and MP2 (1.358 Å) calculations, the microwave gas-phase value (1.354 Å),[30] and an experimental X-ray value (1.364 Å).[31] We also calculated the ^{1}H shielding as a function of C−H bond length for benzene, using C−H bond lengths ranging from 1.08 to 1.105 Å. HF-GIAO shielding calculations were used for all three molecules, and in addition, we used DFT-GIAO with both B3LYP and BPW91 functionals to calculate the ^{19}F shielding in C_6H_5F. The shielding derivatives were expressed in terms of a Taylor series expansion of the shielding as a function of bond length (r):

$$\sigma(r) = \sigma(r_o) + \left(\frac{\partial\sigma}{\partial r}\right)_{r_o}(r - r_o) + \frac{1}{2}\left(\frac{\partial^2\sigma}{\partial r^2}\right)_{r_o}(r - r_o)^2 + \frac{1}{6}\left(\frac{\partial^3\sigma}{\partial r^3}\right)_{r_o}(r - r_o)^3 + \ldots$$

As can be seen in Table 2 (and Tables S4−S8), the first-order shielding derivatives for σ_{33} (along the H−F bond) in HF and for σ_{22} (along the C−H bond in benzene) are very small, with the major shielding changes as a function of bond stretch being perpendicular to the displacement axis, as expected. Surprisingly, however, for the fluorine nucleus in fluorobenzene, the shielding derivative along the C−F bond ($\partial\sigma_{22}/\partial r$) is very large, about 460 ppm/Å, Table 2 and Figure 1, and is essentially independent of the method of calculation, Table 2. While the derivative $\partial\sigma_{22}/\partial r$ is indeed smaller than $\partial\sigma_{33}/\partial r$, Figure 1 and Table 2, the very large first-order shielding derivative along the C−F bond in fluorobenzene means that even relatively small changes in C−F bond length on geometry optimization are likely to make significant contributions to the magnitude to σ_{22}. The observation that σ_{22} is quite susceptible to bond length changes was not expected and neither HF nor the H nuclei in benzene show this effect, which must originate from a strong ^{19}F p-orbital interaction with the benzene ring. This observation therefore raises the possibility that the large improvements in σ_{22} seen in Table 1 on going from an HF- to an MP2-optimized structure might be due primarily to changes in C−F bond length. These results also suggest that geometry optimization may be a more important consideration when calculating individual shielding tensor elements than for the isotropic shifts, as suggested for example from the results shown in Figure 1.

To investigate in more detail the effects of electron correlation and basis sets on the calculation of individual tensor elements, we plotted theoretical vs experimental shielding tensor element results for the seven substituted fluorobenzene molecules, Table 3 (absolute shieldings available in Tables S9−S19). For the MP2-optimized structures, all basis sets used in the HF-GIAO method performed similarly well, with the exception of the D95 basis set, which underestimated σ_{11} and σ_{iso} significantly. The uncoupled DFT-GIAO methods were found to generally overestimate the slope of the individual tensor elements, while predicting the isotropic values with better accord with experiment than did HF-GIAO methods. The coupled SOS-DFPT-IGLO methods computed in deMon-KS3p2 also overestimated the tensor elements, while the isotropic values were in better accord with experiment than either HF-GIAO or MP2-GIAO calculations. The overestimation of shielding tensors via DFT methods has been reported previously for both DFT-GIAO and DFT-IGLO methods.[32,33] Our results also show a general increase in shielding with basis set extension for DFT-GIAO methods, in agreement with the results of Webb et al.[8] Generally, MP2-optimized structures show a larger DFT-GIAO overestimation for each of the tensor elements than does use of an HF-optimized geometry.

More generally, these results indicate that the use of HF methods (geometry optimization and HF-GIAO calculations) give the best overall slope and R^2 values for all tensor elements, although there is more scatter in σ_{22}, Table 3. The results of Table 3 also clearly indicate that the use of the pure density functional, BPW91, overestimates the shielding range, independent of geometry optimization method or basis set, by ∼20−25%. While the isotropic shielding results have less error, this arises from a cancellation of errors in the individual σ_{ii} tensor element calculations. Addition of HF exchange in the hybrid functional, B3LYP, reduces the error, Table 3, but still overestimates the σ_{ii} tensor element range by about 10−20%.

Finally, we consider the orientations of the ^{19}F NMR shielding tensors. Solid state ^{19}F chemical shielding tensor orientations in fluorobenzenes have been determined experimentally in both single crystal[34] and powder[29] samples (from multipulse heteronuclear decoupling experiments). The most shielded component, σ_{33}, was found to be perpendicular to the plane of the benzene ring, while the least shielded component, σ_{11}, was reported to

TABLE 3: Slope and R^2 Values of Experimental[29] vs Theoretical[a] ^{19}F Chemical Shielding Tensor Elements and Isotropic Shift for MP2- and Hartree−Fock-Optimized Fluorobenzenes

				σ_{11}		σ_{22}		σ_{33}		σ_{ii}		σ_{iso}	
program	OPT method	NMR method	basis[b]	slope	R^2	slope	R^2	slope	R^2	slope	R^2	slope	R^2
G98	MP2	HF	1	1.10	0.98	1.10	0.83	0.83	1.00	0.91	0.98	0.83	1.00
G98	MP2	MP2	1	0.80	0.96	0.31	0.15	1.07	1.00	0.91	0.99	0.83	1.00
G98	MP2	DFT-BPW91	1	1.13	0.98	.79	.60	1.07	1.00	1.20	0.99	0.92	0.99
G98	MP2	DFT-B3LYP	1	1.10	0.98	1.16	0.75	1.06	0.99	1.10	0.99	0.85	0.99
G98	MP2	HF	2	1.12	0.99	1.05	0.83	0.83	1.00	0.93	0.98	0.77	0.97
G98	MP2	DFT-BPW91	2	1.16	0.98	0.74	0.57	1.12	1.00	1.23	1.00	0.97	1.00
G98	MP2	DFT-B3LYP	2	1.14	0.98	1.12	0.77	1.09	1.00	1.12	0.99	0.89	0.99
G98	MP2	HF	3	0.76	0.88	1.00	0.84	0.91	0.99	1.12	0.96	0.64	0.94
G98	MP2	HF	4	1.10	0.98	1.10	0.83	0.83	1.00	0.91	0.98	0.83	1.00
deMon	MP2	DFT-PW91	5	1.10	0.98	0.53	0.32	1.12	0.99	1.19	0.99	0.98	1.00
deMon	MP2	DFT-BPW91	5	1.18	0.97	1.11	0.82	.96	1.00	1.15	0.99	0.85	0.99
G98	HF	HF	2	0.97	0.93	0.27	0.09	0.88	0.99	0.98	0.99	0.82	0.97
G98	HF	DFT-BPW91	2	0.90	0.95	0.02	0.00	1.15	0.99	1.29	0.97	0.99	0.90
G98	HF	DFT-B3LYP	2	0.90	0.95	0.46	0.12	1.12	1.00	1.19	0.99	0.97	1.00

[a] The absolute shielding tensors are presented in the Supporting Information, Tables S1−S3 and S9−S19. [b] The basis sets are described in the computational methods: 1, locally dense, 6-311++G(2d,2p)/6-311G 2. 6-311++G(2d,2p); 3, D95; 4, locally dense, 6-311+G(2d)/6-311G(d,p); 5, IGLOIII.

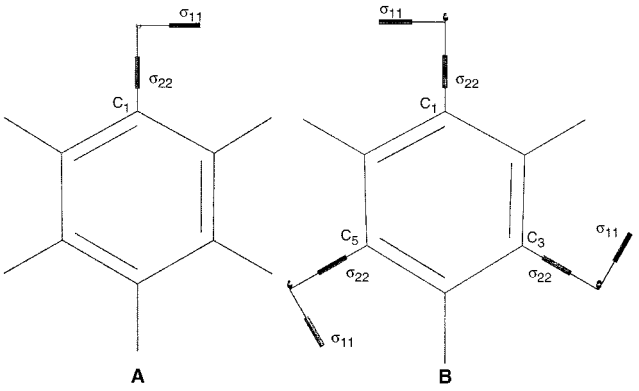

Figure 2. Orientation of the principal components of the ^{19}F shielding tensor elements for (A) monofluorobenzene and (B) 1,3,5-trifluorobenzene as computed by using HF-GIAO on MP2-optimized models.

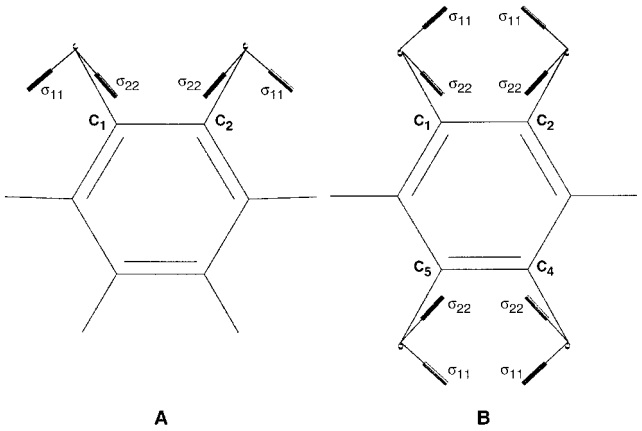

Figure 3. Orientation of the principal components of the ^{19}F shielding tensor elements for (A) 1,2-difluorobenzene and (B) 1,2,4,5-tetrafluorobenzene as computed by using HF-GIAO on MP2-optimized models.

be perpendicular to the C−F bond and σ_{22} to be parallel to the C−F bond axis. The single-crystal result indicated a slight rotation (1°−3°) of σ_{11} and σ_{22} with respect to the C−F bond vector. As shown in Figure 2, our theoretical results are in excellent agreement with experiment for fluorobenzenes lacking ortho neighbors. However, as shown in Figure 3, a slight (∼10°) rotation of σ_{11} and σ_{22} about σ_{33} is seen for fluorobenzenes containing ortho neighbors. Our results also exhibit varying degrees of rotation about σ_{33}, dependent upon the degree of

TABLE 4: Rotation Angle of the ^{19}F Theoretical Shielding Tensor about σ_{33}, the Tensor Element Perpendicular to the Ring Plane[a]

model	atom	angle, deg	model	atom	angle, deg
C_6H_5F	F_1	0	1,2,3,4-$C_6H_2F_4$	$F_{1,4}$	11
1,2-$C_6H_4F_2$	F_1	12	1,2,3,4-$C_6H_2F_4$	$F_{2,3}$	0
1,3-$C_6H_4F_2$	F_1	0	1,2,3,5-$C_6H_2F_4$	$F_{1,3}$	10
1,4-$C_6H_4F_2$	F_1	0		F_2	0
1,2,3-$C_6H_3F_3$	$F_{1,3}$	11		F_5	0
	F_2	0	1,2,4,5-$C_6H_2F_4$	$F_{1,2,4,5}$	14
1,2,4-$C_6H_3F_3$	F_1	12	1,2,3,4,5-C_6HF_5	$F_{1,5}$	13
	F_2	10		$F_{2,4}$	31
	F_4	0		F_3	0
1,3,5-$C_6H_3F_3$	$F_{1,3,5}$	0	C_6F_6	F_{1-6}	0

[a] The angle is measured with respect to the in-plane tensor element that makes the smallest angle with the C−F bond.

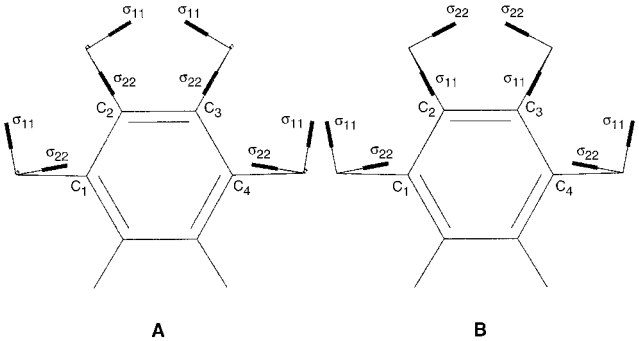

Figure 4. Orientation of the principal components of ^{19}F shielding tensor elements for 1,2,3,4-tetrafluorobenzene as computed by using (A) HF-GIAO and (B) MP2-GIAO methods. The figure shows a switch in the in-plane tensor elements σ_{11} and σ_{22} between theoretical methods.

ortho substitution. The calculated tensor orientations also show a switch in the orientations of σ_{11} and σ_{22} in hexafluorobenzene, with σ_{11} parallel to the C−F bond axis and σ_{22} perpendicular to the C−F bond axis. Each computational method yielded very similar tensor orientations, with the main difference being the degree of rotation about σ_{33} for the ortho-substituted fluorbenzenes, Table 4. The only major difference seen was between HF- and MP2-calculated tensor orientations in 1,2,3,4-tetrafluorobenzene. The HF tensor orientations were in agreement with the single-crystal orientations reported for tetrafluorophthalate,[34] as shown in Figure 4, while the MP2 results showed a switch in σ_{11} and σ_{22} tensor orientation for F_2 (Figure 4).

TABLE 5: Slope and R^2 Values of Experimental[34] vs Theoretical[a] ^{19}F Chemical Shielding Tensor Elements and Isotropic Shift for Tetrafluorophthalate Model Compounds

	method			
	opt	NMR	slope	R^2
model 1	HF	HF	0.84	0.95
model 1	MP2	HF	0.71	0.95
model 1	HF	DFT-IGLO	0.94	0.94
model 1[b]	HF	DFT-IGLO	1.18	0.99
model 2	HF	HF	1.19	0.99
model 3	HF	HF	1.03	0.99
model 3	MP2	HF	0.90	0.98
model 4	HF	HF	0.97	0.99
model 4	MP2	HF	0.91	1.00
model 4	MP2	MP2	1.04	1.00
model 4	HF	DFT-IGLO	1.12	0.99
model 4	MP2	DFT-IGLO	1.25	1.00

[a] The models and methods are as described in the text. [b] These results are from the charge field perturbation calculations.

However, this effect appears to be simply due to the fact that the ^{19}F tensor is essentially axially symmetric in both cases, so even very minor changes in shielding can result in a switch in the ordering of the tensor elements.

In the case of the salt, potassium tetrafluorophthalate, we adopted two different approaches to investigate the F_1 and F_2 shielding tensor magnitudes and orientations. With such ionic species, it is expected to be more difficult to reproduce the experimental results since use of, for example, a single potassium tetrafluorophthalate "molecule" would not adequately reflect the electrostatic field effects and coordination numbers present in the crystal. As expected, initial calculations on the tetrafluorophthalate dianion **1**, provided poor accord with

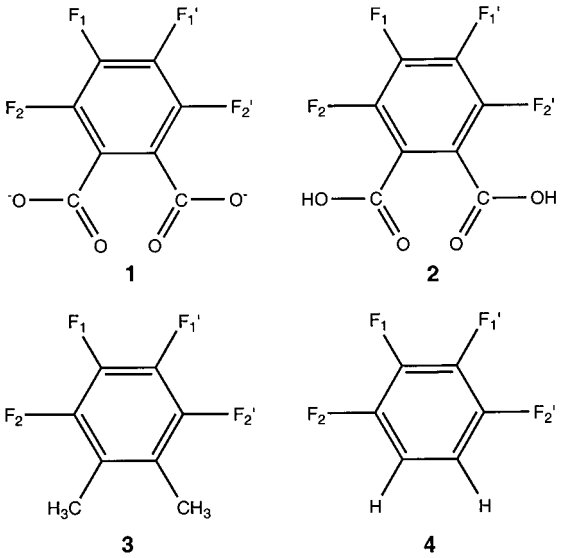

experiment (Table 5); however, use of the diacid **2** or even the model compounds **3** and **4** all provided good agreement with experiment, reproducing the experimentally observed tensor magnitudes (including the "ortho-effect") and orientations quite well, Table 5 and Figure 4A.

The results are model-dependent, and best accord with experiment was achieved by using Hartree−Fock-optimized model **3**, an electroneutral species, in a Hartree−Fock NMR shielding calculation, basically the same result as found for the HF/HF calculations shown in Table 3. Plotting the results of this HF/HF calculation against the experimental results yields a slope of 1.03 and an R^2 value of 0.99, as shown in Figure 5.

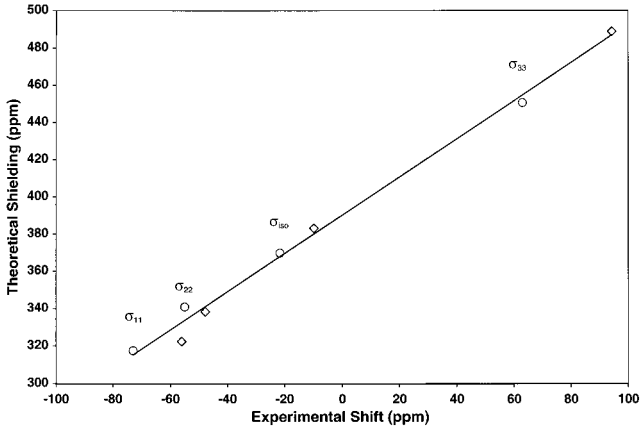

Figure 5. Graph showing correlation between tetrafluorophthalate ^{19}F experimental tensor elements and isotropic shift, and the ^{19}F HF-GIAO theoretical tensor elements and isotropic shielding for 1,2,3,4-tetrafluorobenzene model compound (model **3**). ◇ represents F_1 tensor elements and ○ represents F2 tensor elements. The correlation yields a slope = 1.03 and R^2 = 0.99. Experimental results are from ref 34.

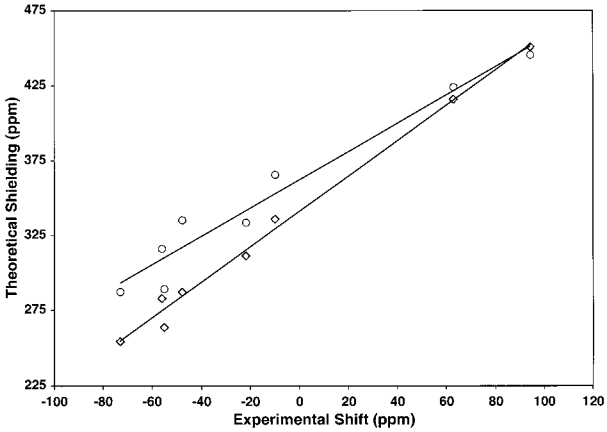

Figure 6. Graph showing the correlation between tetrafluorophthalate dianion ^{19}F experimental tensor elements and isotropic shift and the DFT-IGLO theoretical tensor elements and isotropic shielding for tetrafluorophthalate dianion (model **1**). The model calculation without presence of a charge field is represented by ○; slope = 0.94, R^2 = 0.94. The results represented by ◇ are for the model calculation in the presence of a charge field; slope = 1.18, R^2 = 0.99.

The MP2-optimized MP2-GIAO calculation for model **3** results in a slope of 0.97 with an R^2 of 0.99, while the HF-optimized HF-GIAO results for model **4** are virtually identical to the HF/HF model **3** results, having a slope of 1.04 and an R^2 of 1.0. These results all clearly suggest that the relatively large scatter in model **1** has its origin in the lack of charge balancing counterions. Consequently, we investigated the charge-field perturbation method used previously to evaluate ^{13}C shielding tensors in the zwitterionic amino acids L-threonine and L-tyrosine.[35] In these calculations, we assigned basis functions to a single tetrafluorophthalate dianion (**1**), then surrounded this anion with a charge field derived from point charges representing 53 additonal potassium tetrafluorophthalates, plus two additional charges for the central potassiums. We used the deMon program to compute the shielding tensors for both the isolated tetrafluorophthalate dianion as well as the charge field perturbed species, and results are shown in Table 5 and Figure 6. Clearly, there is a major improvement when using charge field perturbation, with an excellent accord between theory and experiment being found. In addition, the tensor orientations in the CFP model are found to be in better agreement with Griffin's experimental observations[34] than for the tetrafluorophthalate

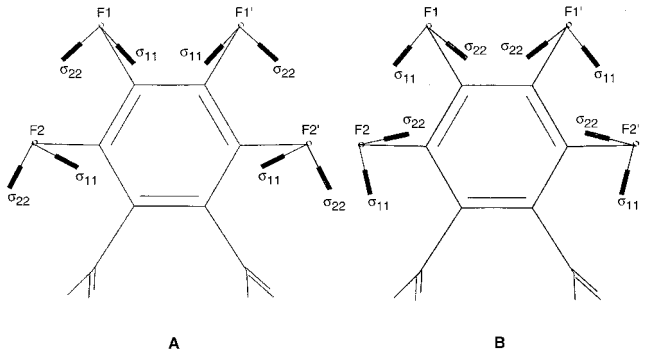

Figure 7. Orientation of the principal components of the ^{19}F shielding tensor elements for (A) tetrafluorothalate dianion and (B) tetrafluorophthalate dianion calculated in the presence of a charge field as computed by using DFT-IGLO on HF-optimized models. The figure shows a switch in the in-plane tensor elements σ_{11} and σ_{22} between theoretical methods.

model calculated without the surrounding charge field. Specifically, as seen in Figure 7, the in-plane components of the shielding tensor switch from σ_{11} oriented along the C−F bond, to σ_{22} oriented along the bond, which agrees with the experimental result.

Conclusions

This investigation of the influence of geometry optimization, electron correlation and basis sets on ^{19}F NMR chemical shielding tensor element calculations is of interest since theoretical methods are now becoming much more frequently used in the interpretation of chemical shifts and in structure determination. This is especially true in biological systems, both in solution and in the solid state, and there is general interest in the question of how best to carry out a given shielding calculation. The results we have obtained show that MP2 geometry optimization has only a relatively small effect on the overall calculation of shielding tensor elements in fluorobenzenes. A possible exception is for σ_{22}, however, it is not clear whether this effect is significant, since the experimental range in σ_{22} is small and is more subject to experimental uncertainty. Variations in C−F bond length appear to account for some of the scatter, since the first-order shielding derivative, $\partial\sigma_{22}/\partial r$, is very large, some 460 ppm Å^{-1}. This was an unexpected result, since in diatomics and for the H nuclei in benzene, tensor elements along the bond (H−F, C−H) direction are not influenced by bond length alterations.

Our results also show that the effects of electron correlation on the calculation of chemical shielding tensors vary, depending on the details of the calculations. MP2-GIAO methods underestimate the in-plane components of shielding, as well as the isotropic shielding, and overestimate the tensor element perpendicular to the ring plane. The inclusion of electron correlation via DFT methods generally showed an overestimation of the tensor elements, while the isotropic shielding was in some cases in better accord with experiment than either HF-GIAO or MP2-GIAO methods. Use of a pure density functional (BPW91) produced the largest errors in slope. As expected, this effect was ameliorated by use of a hybrid functional (B3LYP), although overall the tensor elements were not as well predicted as by using purely HF-GIAO methods. We have also successfully reproduced single-crystal tensor orientations in potassium tetrafluorophthalate and also observed an "ortho-effect" in tensor *orientation* in all substituted fluorobenzenes, resulting in ∼10° rotations of the in-plane tensor elements around σ_{33}.

In summary, the results we have presented above indicate that neither MP2-GIAO nor DFT shielding calculations provide any obvious improvements in theory-versus-experiment correlations of chemical shielding tensor elements in fluorobenzenes over Hartree−Fock methods. Indeed, in systems in which electron correlation is unimportant, as might be expected, pure density functionals and even hybrid functionals perform rather poorly when compared with HF methods. Of course, in systems where electron correlation is expected to be very important, DFT methods may be the method of choice, but for systems such as amino acids in proteins or fluoroaromatic species, it appears that HF methods are quite adequate for investigating both shielding tensor magnitudes and their orientations.

Acknowledgment. This work was supported by the United States Public Health Service (NIH grant GM-50694). We thank Professor D. R. Salahub and Drs. V. Malkin, O. Malkina, and E. Proynov for generously providing their deMon-KS3p2 program. We would also like to thank C. Le and W. D. Arnold for helpful discussions and S. R. Wilson for crystallographic assistance. Computations were carried out in part by use of the SGI/Cray Origin 2000 and HP Exemplar clusters at the National Center of Supercomputing Applications in Urbana, IL (funded in part by the National Computational Science Alliance, grant MCB-000018 N).

Supporting Information Available: The theoretical chemical shielding values for C_6H_6, 1,2-$C_6H_4F_2$, 1,3-$C_6H_4F_2$, 1,4-$C_6H_4F_2$, 1,3,5-$C_6H_3F_3$, 1,2,4,5-$C_6H_2F_4$, and C_6F_6 as calculated via HF-GIAO, MP2-GIAO, DFT-GIAO, and DFT-IGLO methods are presented in Tables S1−S19. This material is available free of charge via the Internet at http://pubs.acs.org.

References and Notes

(1) Luck, L. A.; Falke, J. J. *Biochemistry* **1991**, *30*, 4248−4256.
(2) Lian, C.; Le, H.; Montez, B.; Patterson, J.; Harrell, S.; Laws, D.; Matsumura, I.; Pearson, J.; Oldfield, E. *Biochemistry* **1994**, *33*, 5238−5245.
(3) de Dios, A. C.; Oldfield, E. *J. Am. Chem. Soc*. **1994**, *116*, 7453−7454.
(4) Arnold, W. D.; Mao, J.; Sun, H.; Oldfield, E. *J. Am. Chem. Soc*. **2000**, *122*, 12164−12168.
(5) Ditchfield, R. *Mol. Phys*. **1974**, *27*, 789−807.
(6) Wolinski, K.; Hinton, J. F.; Pulay, P. *J. Am. Chem. Soc*. **1990**, 8251−8260.
(7) Karadakov, P. B.; Webb, G. A.; England, J. A. *Modeling NMR Chemical Shifts − Gaining Insights into Structure and Environment*; Facelli, J. C., deDios, A. C., Eds.; ACS Symposium Series 732; American Chemical Society: Washington, DC, 1999; pp 115−125.
(8) Webb, G. A.; Kardakov, P. B.; England, J. A. *Bull. Pol. Acad. Sci. Chem.* **2000**, *48*, 101−112.
(9) Fukui, H. *Prog. Nucl. Magn. Res. Spectrosc.* **1997**, *32*, 317−342.
(10) St-Amant, A.; Salahub, D. R. *Chem. Phys. Lett*. **1990**, *169*, 387−392.
(11) St-Amant, A. Ph.D. Thesis, Université de Montréal, 1992.
(12) Casida, M. E.; Paul, C. D.; Goursot, A.; Koester, A.; Petterson, L.; Proynov, E.; St-Amant, A.; Salahub, D. R.; Duarte, H.; Godbout, N.; Guan, J.; Jamorski, C.; Leboeuf, M.; Malkin, V.; Malkina, O.; Sim, F.; Vela, A. *deMon-KS*, version 3.2; deMon Software, Université de Montréal: Montreal, 1997.
(13) Møller, C.; Plesset, M. S. *Phys. Rev*. **1934**, *46*, 618−622.
(14) Gauss, J. *Chem. Phys. Lett*. **1992**, *191*, 614−620.
(15) Gauss, J. *J. Chem. Phys*. **1993**, *99*, 3629−3643.
(16) Wolfram, K.; Holthausen, M. C. *A Chemist's Guide to Density Functional Theory*; Wiley-VCH: Weinheim, 2000; pp 195−212.
(17) Frisch, M. J.; Trucks, G. W.; Schlegel, H. B.; Scuseria, G. E.; Robb, M. A.; Cheeseman, J. R.; Zakrzewski, V. G.; Montgomery, J. A. Jr.; Stratmann, R. E.; Burant, J. C.; Dapprich, S.; Millam, J. M.; Daniels, A. D.; Kudin, K. N.; Strain, M. C.; Farkas, O.; Tomasi, J.; Barone, V.; Cossi, M.; Cammi, R.; Mennucci, B.; Pomelli, C.; Adamo, C.; Clifford, S.; Ochterski, J.; Petersson, G. A.; Ayala, P. Y. Cui, Q.; Morokuma, K.; Malick, D. K.; Rabuck, A. D.; Raghavachari, K.; Foresman, J. B.; Cioslowski, J.; Ortiz, J. V.; Baboul, A. G.; Stefanov, B. B.; Liu, G.; Liashenko, A.; Piskorz, P.; Komaromi, I.; Gomperts, R.; Martin, R. L.; Fox, D. J.; Keith, T.; Al-

Laham, M. A.; Peng, C. Y.; Nanayakkara, A.; Gonzalez, C.; Challacombe, M.; Gill, P. M. W.; Johnson, B.; Chen, W.; Wong, M. W.; Andres, J. L.; Gonzalez, C.; Head-Gordon, M.; Replogle, E. S.; Pople, J. A. *Gaussian 98*, revision A.7; Gaussian, Inc.: Pittsburgh, PA, 1998.

(18) Hehre, W. J.; Radom, L.; Schleyer, P. V. R.; Pople, J. A. *Ab Initio Molecular Orbital Theory*; John Wiley: New York, 1986.

(19) Kutzelnigg, W.; Fleischer, U.; Schindler, M. In *NMR Basic Principles and Progress*; Diehl, P., Fluck, E., Gunther, H., Kosfeld, R., Seelig, J., Eds.; Springer-Verlag: Berlin, 1990; Vol. 23, pp 165−262.

(20) Becke, A. D. *Phys. Rev. A* **1988**, *38*, 3098−3100.

(21) Perdew, J. P.; Wang, Y. *Phys. Rev. B* **1986**, *33*, 8800−8802.

(22) Perdew, J. P.; Wang, Y. *Phys. Rev. B* **1992**, *45*, 13244−13249.

(23) Becke, A. D. *J. Chem. Phys.* **1993**, *98*, 5648−5652.

(24) Lee, C.; Yang, W.; Parr, R. G. *Phys. Rev. B* **1988**, *37*, 785−789.

(25) Chestnut, D. B.; Moore, K. D. *J. Comput. Chem*. **1989**, *10*, 648−659.

(26) deDios, A. C.; Pearson, J. G.; Oldfield, E. *Science* **1993**, *260*, 1491−1496.

(27) de Dios, A. C.; Oldfield, E. *Chem. Phys. Lett*. **1993**, *205*, 108−116.

(28) Dauber-Osguthorpe, P.; Roberts, V. A.; Osguthorpe, D. J.; Wolff, J.; Genest, M.; Hagler, A. T. *Proteins: Struct., Function Genet.* **1998**, *4*, 31−47.

(29) Raber, H.; Mehring, M. *Chem. Phys.* **1977**, *26*, 123−130.

(30) Nygaard, L.; Bojesen, I.; Pedersen, T.; Rastrup-Andersen, J. J. *J. Mol. Struct*. **1968**, *2*, 209−215.

(31) Thalladi, V. R.; Weiss, H.-C.; Bläser, D.; Boese, R.; Nangia, A.; Desiraju, G. R. *J. Am. Chem. Soc.* **1998**, *120*, 8702−8710.

(32) Cheeseman, J. R.; Trucks, G. W.; Keith, T. A.; Frisch, M. J. *J. Chem Phys*. **1996**, *104*, 5497−5509.

(33) Havlin, R.; McMahon, M.; Srinivasan, R.; Le, H.; Oldfield, E. *J. Phys. Chem. A* **1997**, *101*, 8908−8913.

(34) Griffin, R. G.; Yeung, H. N.; LaPrade, M. D.; Waugh, J. S. *J. Phys. Chem*. **1973**, *59*, 777−783.

(35) de Dios, A. C.; Laws, D. D.; Oldfield, E. *J. Am. Chem. Soc*. **1994,** *116*, 7784−7786.